PROCEEDINGS OF SCIENCE

Rare Higgs Decays in the Standard Model

Xi Gong[a,b,*]

[a] *Interdisciplinary Center for Theoretical Study, University of Science and Technology of China, Hefei, Anhui 230026 China*

[b] *Peng Huanwu Center for Fundamental Theory, Hefei, Anhui 230026 China*

E-mail: gonff@mail.ustc.edu.cn

Motivated by the recent experiments at LHC, we have presented the theoretical analysis of rare processes, including Higgs decays into lepton pair plus one light hadron and decays into a pair of heavy vector quarkonia, in the standard model. Hopefully, experimental studies of these very rare decays in future high-precision experimental facilities might be interesting both to test the standard model and to look for new physics scenarios.

The Tenth Annual Conference on Large Hadron Collider Physics - LHCP2022
16-20 May 2022
online

*Speaker

© Copyright owned by the author(s) under the terms of the Creative Commons Attribution-NonCommercial-NoDerivatives 4.0 International License (CC BY-NC-ND 4.0). https://pos.sissa.it/

PoS(LHCP2022)250

1. Introduction

After the discovery of Higgs boson by the ATLAS and CMS Collaborations [1], a new era of the precise determination of the properties of this new particle has begun. In recent years, experimental searches for rare Higgs decays, like $h \to V\gamma$ [2] (V denotes vector mesons ρ, ϕ, J/Ψ and Υ etc.), and $h \to VV$ [3] ($V = J/\Psi, \Upsilon$) have been performed at the LHC. Motivated by the above experimental studies, we have presented the theoretical analysis of rare processes, including Higgs decays into lepton pair plus one light hadron [4] and decays into a pair of heavy vector quarkonia [5], in the standard model (SM).

2. $h \to V\ell\bar{\ell}$

In the SM, the $h \to V\ell\bar{\ell}$ decays will get contribution from the diagrams, as shown in Figure 1.

To illustrate the numerical results for branching fractions, we normalize these decay rate to the theoretical prediction for the total Higgs width in the SM, $\Gamma_h = 4.10$ MeV, referring to $m_h = 125.09$ GeV [6]. The results are as following

$\mathcal{B}(h \to \rho^0 e^+ e^-)$	$(4.61 \pm 0.06) \times 10^{-7}$	$\mathcal{B}(h \to \pi^0 e^+ e^-)$	$(7.06 \pm 0.02) \times 10^{-8}$
$\mathcal{B}(h \to \rho^0 \mu^+ \mu^-)$	$(3.97 \pm 0.05) \times 10^{-7}$	$\mathcal{B}(h \to \pi^0 \mu^+ \mu^-)$	$(7.06 \pm 0.02) \times 10^{-8}$
$\mathcal{B}(h \to \rho^0 \tau^+ \tau^-)$	$(1.80 \pm 0.02) \times 10^{-5}$	$\mathcal{B}(h \to \pi^0 \tau^+ \tau^-)$	$(7.10 \pm 0.02) \times 10^{-8}$
$\mathcal{B}(h \to \omega e^+ e^-)$	$(4.17 \pm 0.09) \times 10^{-8}$	$\mathcal{B}(h \to \pi^0 \nu\bar{\nu})$	$(4.21 \pm 0.01) \times 10^{-7}$
$\mathcal{B}(h \to \omega \mu^+ \mu^-)$	$(3.61 \pm 0.08) \times 10^{-8}$	$\mathcal{B}(h \to \pi^+ \ell^- \bar{\nu}_\ell)$	$(4.05 \pm 0.01) \times 10^{-7}$
$\mathcal{B}(h \to \omega \tau^+ \tau^-)$	$(1.58 \pm 0.03) \times 10^{-6}$	$\mathcal{B}(h \to \rho^+ \ell^- \bar{\nu}_\ell)$	$(1.03 \pm 0.01) \times 10^{-6}$
$\mathcal{B}(h \to \rho^0 \nu\bar{\nu})$	$(1.19 \pm 0.01) \times 10^{-6}$	$\mathcal{B}(h \to K^+ \ell^- \bar{\nu}_\ell)$	$(3.14 \pm 0.01) \times 10^{-8}$
$\mathcal{B}(h \to \omega \nu\bar{\nu})$	$(1.11 \pm 0.02) \times 10^{-7}$	$\mathcal{B}(h \to K^{*+} \ell^- \bar{\nu}_\ell)$	$(5.32 \pm 0.02) \times 10^{-8}$

The dilepton invariant mass distribution and the angular distribution of $h \to \rho^0 \ell^+ \ell^-$ decay have been displayed in Figure 2 for $\ell = e, \mu$, and τ, respectively. From these plots, one can readily find that, the contribution from the Higgs coupling to leptons [Figure 1(b)] is vanishingly small for the electron mode, and could be relevant in the muon case; while

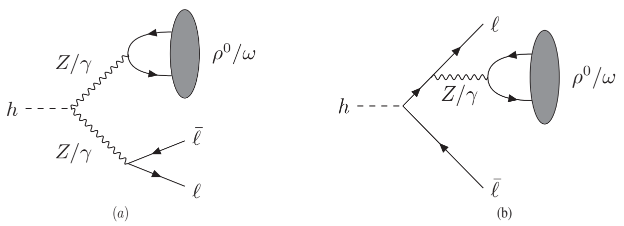

Figure 1: Lowest-order diagrams for $h \to V\ell\bar{\ell}$ ($V = \rho^0, \omega$) decays in the SM. The virtual photon γ or Z can also be emitted from $\bar{\ell}$ line in the diagram (b). After some adjustment, by omitting some terms, it also gives the decay amplitudes for $h \to \pi^0 \ell\bar{\ell}$, $h \to \pi^+(K^+)\ell^- \bar{\nu}_\ell$, and $h \to \rho^+(K^{*+})\ell^- \bar{\nu}_\ell$.

PoS(LHCP2022)250

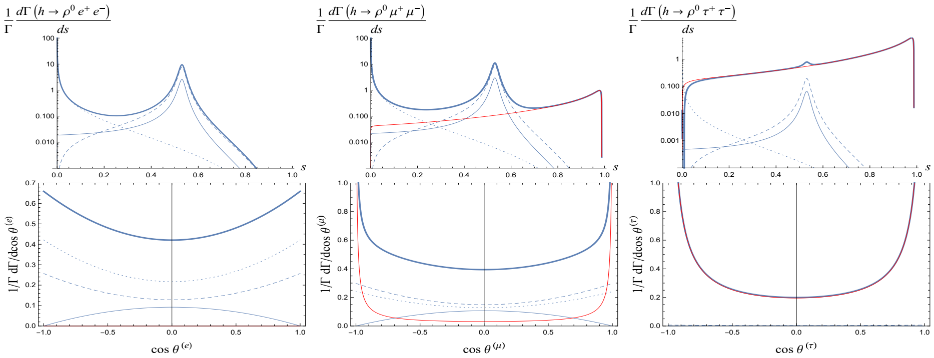

Figure 2: The normalized invariant mass distribution and angular distribution of $h \to \rho^0 \ell^+ \ell^-$ decay for $\ell = e, \mu$, and τ, respectively. The thin solid line denotes the contribution from hZZ, the dashed line from $hZ\gamma$, the dotted line from $h\gamma\gamma$, the red line from Figure 1(b) via the virtual photon only while the thick solid line gives the total contribution.

it is dominant, giving about 99% contribution, thus leads to larger rate for the $\tau^+\tau^-$ final state.

On the other hand, one can find that the contributions from hZZ and $hZ\gamma$ vertices are of the same importance. It is interesting to note that, in the SM, the $hZ\gamma$ and $h\gamma\gamma$ couplings are loop-induced while hZZ and the Higgs coupling to leptons are the tree-level vertices. This seems to indicate that $h \to \rho^0 \ell^+ \ell^-$ with $\ell = e$ and μ could be sensitive to the short-distance physics and studies of these decays may help to probe the novel dynamics in the Higgs sector.

3. $h \to VV$

Figure 3 and Figure 4 show the diagrams of $h \to VV$ processes in the SM. Figure 3 gives transitions where the final states are longitudinally polarized, and Figure 4 transversely polarized. By adopting the nonrelativistic color-singlet model [7], one can get the numerical results as shown in Table 1.

Compared to the process of longitudinally polarized final states, the transeversely polarized final states have a $\epsilon^*(p) \cdot \epsilon^*(q) \sim m_V^2/m_h^2$ suppression, due to the polarization structure. However, the photon propagator can give a $1/m_V^2$ factor, which can counteract

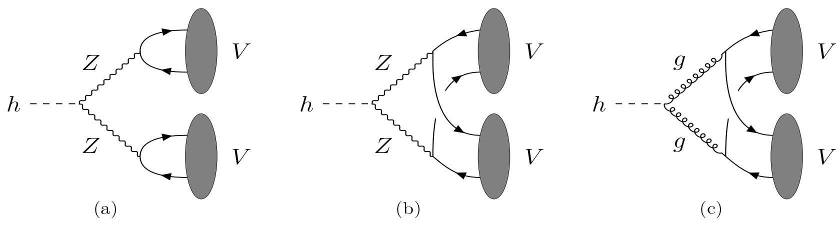

Figure 3: $h \to VV$ decays in the SM: (a) and (b) through the ZZ intermediate state while (c) through the gluon intermediate state.

PoS(LHCP2022)250

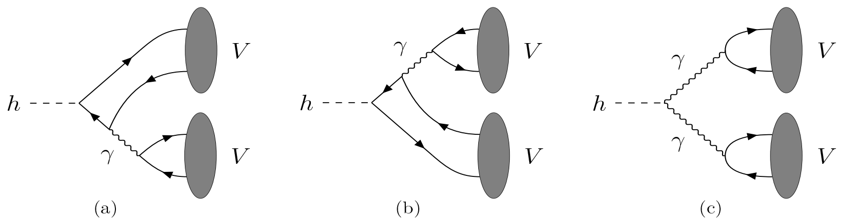

Figure 4: $h \to VV$ decays in the SM through the virtual photon intermediate states.

V	m_V(GeV)	$\mathcal{B}_1(h \to VV)$	$\mathcal{B}_2(h \to VV)$	$\mathcal{B}(h \to VV)$
$J/\Psi(1S)$	3.097	$(1.6 \pm 0.6) \times 10^{-11}$	$(5.8 \pm 2.2) \times 10^{-10}$	$(5.9 \pm 2.3) \times 10^{-10}$
$\Psi(2S)$	3.686	$(3.9 \pm 1.5) \times 10^{-12}$	$(4.7 \pm 1.8) \times 10^{-11}$	$(5.1 \pm 2.0) \times 10^{-11}$
$\Upsilon(1S)$	9.460	$(4.1 \pm 0.8) \times 10^{-10}$	$(2.4 \pm 0.5) \times 10^{-11}$	$(4.3 \pm 0.9) \times 10^{-10}$
$\Upsilon(2S)$	10.02	$(9.6 \pm 1.9) \times 10^{-11}$	$(6.4 \pm 1.3) \times 10^{-12}$	$(1.0 \pm 0.2) \times 10^{-10}$
$\Upsilon(3S)$	10.36	$(5.4 \pm 1.1) \times 10^{-11}$	$(3.8 \pm 0.8) \times 10^{-12}$	$(5.7 \pm 1.2) \times 10^{-11}$

Table 1: Branching ratios of $h \to VV$ decays with V denoting the narrow $c\bar{c}$ and $b\bar{b}$ heavy vector quarkonia.

the above suppression. For charmonium case, transversely polarized final states give dominant contributions; while for bottomonium modes, the longitudinally polarized ones are more important.

4. Summary

Exclusive rare Higgs decays into lepton pair plus one light hadron, such as $h \to \rho^0(\omega)\ell\bar{\ell}$, $h \to \pi^0\ell\bar{\ell}$, $h \to \pi^+(K^+)\ell^-\bar{\nu}_\ell$, and $h \to \rho^+(K^{*+})\ell^-\bar{\nu}_\ell$, have been explored in the standard model. Decay amplitudes are dominantly from the Higgs couplings to gauge bosons and to charged leptons, and their branching ratios are predicted in the range of $10^{-8} \sim 10^{-5}$. We have also analyzed the differential dilepton invariant mass and angular distributions of $h \to \rho^0\ell^+\ell^-$ decays.

Higgs decays into pair of heavy quarkonia, $h \to VV$, has also been explored in the SM. The total decay rates of $h \to VV$ in the SM have also been calculated, and our predictions for their branching fractions are around 10^{-10}. The transversely polarized final states can also give important contributions.

It will be chanllenging to search for these rare processes. Nevertheless, experimental studies of them, might be interesting both to help deepen our understanding of the standard model and to probe new physics beyong the standard model in the future high-precision experiments.

This work was supported in part by the National Natural Science Foundation of China under Grants No. 11575175 and No. 12047502, and by National Research and development Program of China under Contract No. 2020YFA0406400.

PoS(LHCP2022)250

References

[1] ATLAS Collaboration, G. Aad et al., Phys. Lett. B **716** (2012) 1; CMS Collaboration, S. Chatrchyan et al., Phys. Lett. B **716** (2012) 30.

[2] ATLAS Collaboration, G. Aad et al., Phys. Rev. Lett. **114** (2015) 121801, arXiv: 1501.03276 [hep-ex]; ATLAS Collaboration, M. Aaboud et al., Phys. Rev. Lett. **117** (2016) 111802, arXiv: 1607.03400 [hep-ex].

[3] CMS Collaboration, A.M. Sirunyan et al., Phys. Lett. B **797** (2019) 134811, arXiv: 1905.10408 [hep-ex].

[4] D. N. Gao and X. Gong, Phys. Lett. B **817**, 136348 (2021) [arXiv:2103.03050 [hep-ph]].

[5] D. N. Gao and X. Gong, Phys. Lett. B **832**, 137243 (2022) [arXiv:2203.00514 [hep-ph]].

[6] LHC Higgs Cross Section Working Group, *Handbook of LHC Higgs Cross Sections: 4. Deciphering the nature of the Higgs sector*, arXiv: 1610.07922 [hep-ph].

[7] T. Appelquist and H. Politzer, Phys. Rev. Lett. **34**, 43 (1975); A. De Rujula and S.L. Glashow, Phys. Rev. Lett. **34**, 46 (1975); J.H. Kühn, J. Kaplan, and E. Safiani, Nucl. Phys. B **157** (1979) 125; C. H. Chang, Nucl. Phys. B **172** (1980) 425; W.Y. Keung, Phys. Rev. D **23** (1981) 2072; E.L. Berger and D. Jones, Phys. Rev. D **23** (1981) 1521; L. Clavelli, Phys. Rev. D **26** (1982) 1610; L. Clavelli, T. Gajdosik, and I. Perevalova, Phys. Lett. B **523** (2001) 249, hep-ph/0110076; L. Clavelli, P. Coulter, and T. Gaidosik, Phys. Lett. B **526** (2002) 360, hep-ph/0111250.

PoS(LHCP2022)250